PAPER • OPEN ACCESS

Elephant trunks use an adaptable prehensile grip

To cite this article: Andrew K Schulz et al 2023 Bioinspir. Biomim. 18 026008

View the article online for updates and enhancements.

You may also like

- ORION'S VEIL: MAGNETIC FIELD STRENGTHS AND OTHER PROPERTIES OF A PDR IN FRONT OF THE TRAPEZIUM CLUSTER T. H. Troland, W. M. Goss, C. L. Brogan et al
- Research regarding stiffness optimization of wires used for joints actuation from an elephant's trunk robotic arm C Ciofu and G Stan
- HUBBLE SPACE TELESCOPE IMAGES AND FOLLOW-UP SPECTROSCOPY OF THE ORION NEBULA C. R. O'dell, Zheng Wen and J. J. Hester

Bioinspiration & Biomimetics

OPEN ACCESS



6 October 2022

REVISED

4 January 2023

ACCEPTED FOR PUBLICATION 18 January 2023

PURIISHED

8 February 2023

Original content from this work may be used under the terms of the Creative Commons Attribution 4.0

Any further distribution of this work must maintain attribution to the author(s) and the title of the work, journal citation and DOI.



PAPER

Elephant trunks use an adaptable prehensile grip

Andrew K Schulz^{1,2}, Joy S Reidenberg³, Jia Ning Wu⁷, Cheuk Ying Tang⁴, Benjamin Seleb⁵, Josh Mancebo⁶, Nathan Elgart⁶ and David L Hu^{1,5,*}

- Schools of Mechanical Engineering, Georgia Institute of Technology, Atlanta, GA 30332, United States of America
- Max Planck Institute for Intelligent Systems, Stuttgart, Germany
- Center for Anatomy and Functional Morphology, Icahn School of Medicine at Mount Sinai, New York, NY, United States of America
- Radiology, Neuroscience, & Psychiatry Translation and Molecular Imaging Institute, Icahn School of Medicine at Mount Sinai, New York, NY, United States of America
- Biological Sciences, Georgia Institute of Technology, Atlanta, GA 30332, United States of America
- Zoo Atlanta, Atlanta, GA 30315, United States of America
- School of Additive Manufacturing, Sun Yat-Sen University, Shenzhen, People's Republic of China
- Author to whom any correspondence should be addressed.

E-mail: hu@me.gatech.edu

Keywords: weight lifting, power, capstan

Supplementary material for this article is available online

Abstract

Elephants have long been observed to grip objects with their trunk, but little is known about how they adjust their strategy for different weights. In this study, we challenge a female African elephant at Zoo Atlanta to lift 20–60 kg barbell weights with only its trunk. We measure the trunk's shape and wrinkle geometry from a frozen elephant trunk at the Smithsonian. We observe several strategies employed to accommodate heavier weights, including accelerating less, orienting the trunk vertically, and wrapping the barbell with a greater trunk length. Mathematical models show that increasing barbell weights are associated with constant trunk tensile force and an increasing barbell-wrapping surface area due to the trunk's wrinkles. Our findings may inspire the design of more adaptable soft robotic grippers that can improve grip using surface morphology such as wrinkles.

1. Introduction

In this study, we investigate the elephant trunk's prehension, the ability to grasp or seize by wrapping around [1]. Prehension has evolved many times in both animals and plants to enable an organism to grasp vegetation. Examples include elephant trunks, giraffe tongues, plant tendrils, monkey tails, and the human hand. While prehensile behavior has long been noted in these organisms, few systematic studies exist because the action is often fast and performed in treetops. In comparison, elephants are terrestrial, highly trainable, and have an enormous range of weights they can lift. Thus, elephants are ideal for studying the mechanics of prehensile grip.

One of the earliest studies of elephant trunk biomechanics was a 1991 study of an Asian elephant lifting a kettlebell-style weight. Based on the bending of the trunk during the lift, the authors showed the trunk had an effective modulus of elasticity of 985 kPa [2]. Similar to how fish suck prey into their mouths, elephants inhale to grab nearby items such as tortilla chips [3]. They can use their trunk 'fingers,' the prehensile tips of their trunk, to pack together a series of items for a single pickup [4]. Although the range of movements appears complex, the trunk's motion can be simplified to a set of 17 basic motion primitives [5]. These primitives were discovered by 3D tracking two adult male elephants grasping objects of varying shape and mass [5]. In this study, we provide an elephant with identically sized but variously weighted dumbbells to isolate how the elephant changes its gripping strategy.

We next review work on prehension in monkeys and the human hand in order to obtain some context for elephant prehension. Prehensile tails are thought to have evolved in dense South American forests, where animals often traverse narrow supports and distribute their weight to the surrounding canopy [6, 7]. The most well-known examples of prehensile animals are the Atelinae, a subfamily of monkeys that includes howler and spider monkeys [8]. Both spider and howler monkeys can hang their entire body weight (up to 10 kg) from their tail, a behavior that frees their hands to manipulate fruit [9]. This feat requires specialized anatomy such as substantial musculature, innervation to control the tail, and a particular region in the brain for tail control. Another adaptation that makes these monkeys more prehensile than the capuchins is their friction pad, a hairless and highly sensitive strip of skin on their tail [10]. In contrast, capuchins have a tail that is covered in fur. Due to their quick movement through the dense canopy, there are few measurements of tail prehension [11]. Instead of a smooth friction pad as in capuchins, elephants have had a wrinkled ventral section in their trunk [12]. In this study, we consider how wrinkles may increase the surface area of the grip.

Much of the neuroscience of prehensile gripping was found by studying humans. Many tools in the human-built world, such as knobs, steering wheels, and door handles, were designed to be operated by the human hand. Thus, robot designers have shown a keen interest in mimicking the human hand [13]. The human hand has five fingers, over 25 degrees of freedom, and three grasping motor primitives (transverse, perpendicular, or parallel to the palm). Motor primitives are described as neural mechanisms that assist with coordinated motions. Different postures present varying degrees of force, motion, and sensory information [13]. Like the human hand, the African elephant trunk can move with precision and high force due to its 60 000 facial neurons [14].

Elephant trunks and other soft biological structures have been sources of inspiration for soft robotic manipulators for the past twenty years [15–18]. A novel way of actuating soft robots is through robotic skins, which use pneumatics to move previously inanimate objects [19]. Robotic skins can be used for both actuation, and sensation [20]. Snakes are also prehensile, and their ability to climb trees relies in part on the dynamics of their ventral scales, which can be angled like venetian blinds to increase friction [21]. Bio-inspired robots with actuated ventral scales can climb inclined surfaces using similar mechanisms to snakes [22]. In this work, we will observe how the elephant trunk can make contact with objects using wrinkles along its trunk.

2. Materials and methods

2.1. Elephant experiments

We initially attempted to train two female elephants at Zoo Atlanta, but only one elephant was receptive. Experiments are thus reported for one elephant 35 year-old female African Elephant (*Loxodonta* africana) of mass 3360 kg and height 2.6 m. We conducted experiments outdoors, at the edge of the elephant's enclosure at Zoo Atlanta. The experiments occurred over two-hour periods in the mornings of spring and summer 2018 before Zoo Atlanta opened to the public. The staff at Zoo Atlanta supervised all experiments.

To train the elephant to lift, the zookeepers used a reward system beginning with gesturing the elephant towards the barbell (figure 1(b)). If the elephant accomplished the correct task of grabbing and lifting the bar, food was rewarded (figures 1(c) and (d)). If an incorrect outcome was observed, then the experimental procedure was repeated until the trial was successful. Once an 80% success rate was achieved, we commenced weightlifting experiments (figure 2(a)). It took 15 attempts and 10 min of training to accomplish an 80% success rate.

Experiments were conducted with a Smith Machine (Powerline PSM144X, $2.0 \times 1.1 \times 1.9$ m), which uses twin frictionless carriages to constrain the barbell to move vertically. The barbell was placed at a set distance of $w = 0.5 \pm 0.05$ m (n = 22) away from the enclosure bars. As a result of this distance, the elephant had to rely on its trunk to lift. Without the restraint of the bars, the elephant would likely use a combination of its forehead, trunk, and tusks to lift heavy objects.

Iron weight plates were added to the 20-kg bar to provide the elephant a set of six weights comprising 20, 25, 30, 35, 43, and 60 kg. Note the 43-kg mass results from a 45-pound bar with two 25-pound weights added. The elephant completed four trials of each weight, with each successful trial ending in a food reward and one-minute rest between each lift. When weights were changed, five minutes of rest were given to change the weights and resecure the frame to the ground using 80-kg of barbell weights.

Twenty-two barbell lifts were filmed using a high-definition digital video camera (Sony HDRXR200) and iPhone 8. We tracked the position of the weight along the 2.0 m height of the Smith machine to accurately determine the barbell height. In two trials, the elephant barely lifted the bar above its original position; such experiments were considered incomplete, and the data were not analyzed. Analysis of the elephant lifting 50 kg was removed from the analysis because the elephant broke the Smith machine during the 50 kg test. During testing, the elephant struggled to lift the 60 kg barbell and only proceeded to lift it twice.

We tracked the trunk tip shape by first drawing along a line of chalk on the mid-line of the right lateral side of the elephant trunk. Using Tracker, an open-source video analysis tool (https://physlets.org/tracker/), we tracked 60 equally spaced points along this line. The speed and acceleration of the elephant lift were determined by tracking the barbell side-view

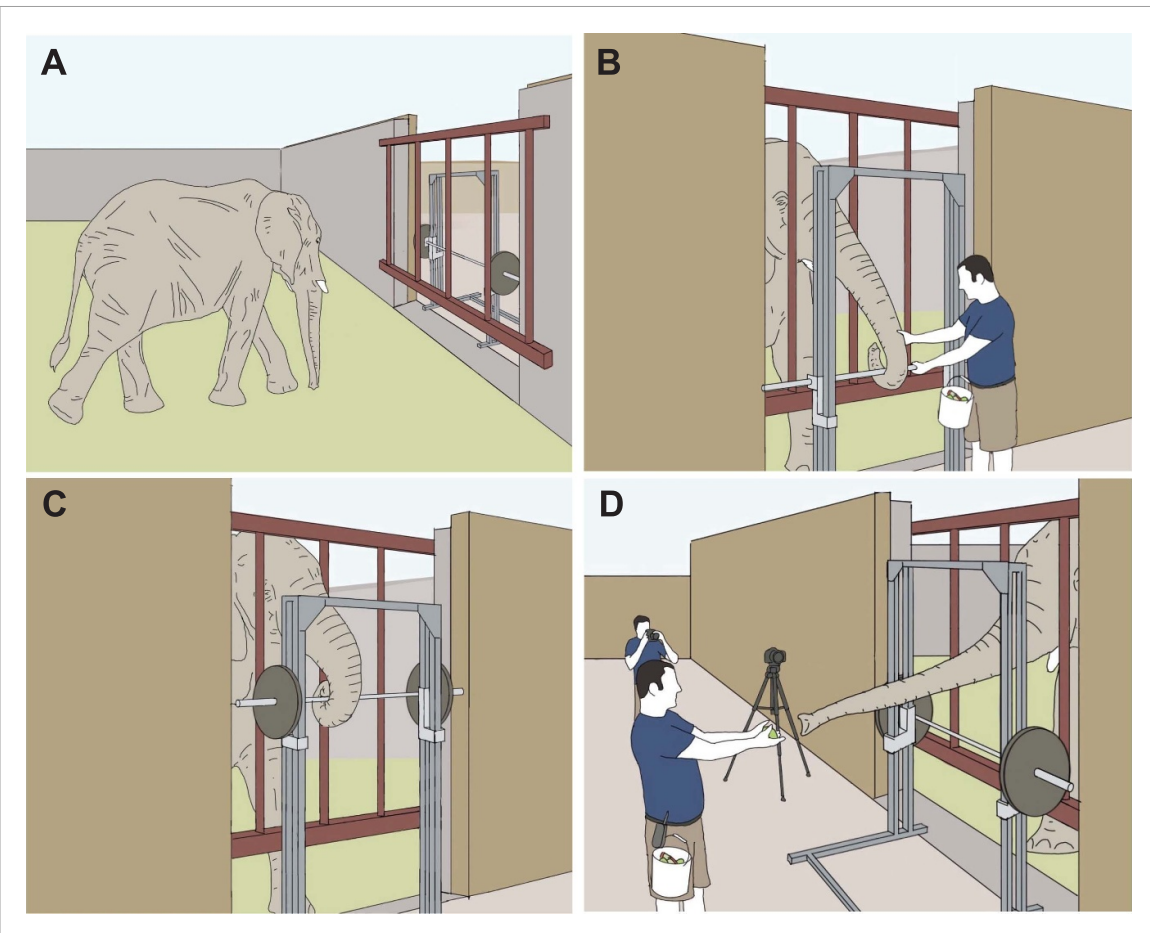


Figure 1. Procedures for elephant lifting the barbell. (a) The African elephant *Loxodonta africana* approaches the barbell setup. (b) A Zoo Atlanta elephant keeper instructs the elephant how to wrap its trunk around the barbell and lift. (c) Elephant completing a trial with a heavier weight. (d) After completing a trial, the elephant reaches out to Zoo Atlanta keeper for a food incentive. Illustrations by Benjamin Seleb.

position. Tracking the trunk's base was impossible because the elephant's head rose out of the frame.

2.2. Dissection of an elephant trunk

Icahn School of Medicine at Mount Sinai, New York provided access to a frozen trunk from a 38-year-old female African elephant, Loxodonta africana, that initially lived in a Virginia zoo. Detailed information about the elephant can be found in the pathology report (supplemental figure 1). The elephant's body weight before death was approximately 4000 kg, and the weight, age, and sex of the elephant were comparable to those of the elephant filmed in our study. The trunk was cut into several parts and stored in a freezer in 2015 at -15 °C until we dissected it in July 2016. In January 2018, the specimen's distal tip was fully thawed and scanned on a Siemens Dual Source Force CT to measure the trunk's nasal passageways and outer diameter. A helical scan was performed with 80 kV, 183 mAs, a slice thickness of 0.5 mm, an acquisition speed of 737 mm s^{-1} , and a temporal resolution of 66 ms (figures 3(a) and (b), supplemental video 4). We scanned the distal portion of the trunk up to around 110 cm from the tip. That was as much of the trunk as that could fit in the CT scanner.

We obtained 27 measurements of the trunk's inner diameter as the scan progressed from the proximal root to the distal tip (figure 4(c)). We also rendered the entire CT image of the trunk to see the three-dimensional structure (supplemental video 5).

3. Mathematical modeling

3.1. Elephant trunk geometry

We modeled both the elephant trunk and its nasal cavities as conical frustums [23]. Assuming the mass density of the trunk is $\rho = 1180 \text{ kg m}^{-3}$, measured from a cross-section of an elephant carcass' trunk [2], the mass m_t of a trunk segment of length z may be modeled using a solid frustum with two hollow frustums as nasal cavities. With these assumptions, the mass may be written [24]:

$$m_t(z) = \frac{\pi \rho z}{3} \left[R^2(z) + R(z)R(0) + R^2(0) -2 \left(r^2(z) + r(z)r(0) + r^2(0) \right) \right].$$
 (1)

The length z is measured from the trunk tip, and R(z) and r(z) are, respectively, the outer and inner radii of the trunk at a position z. Based on the frozen trunk

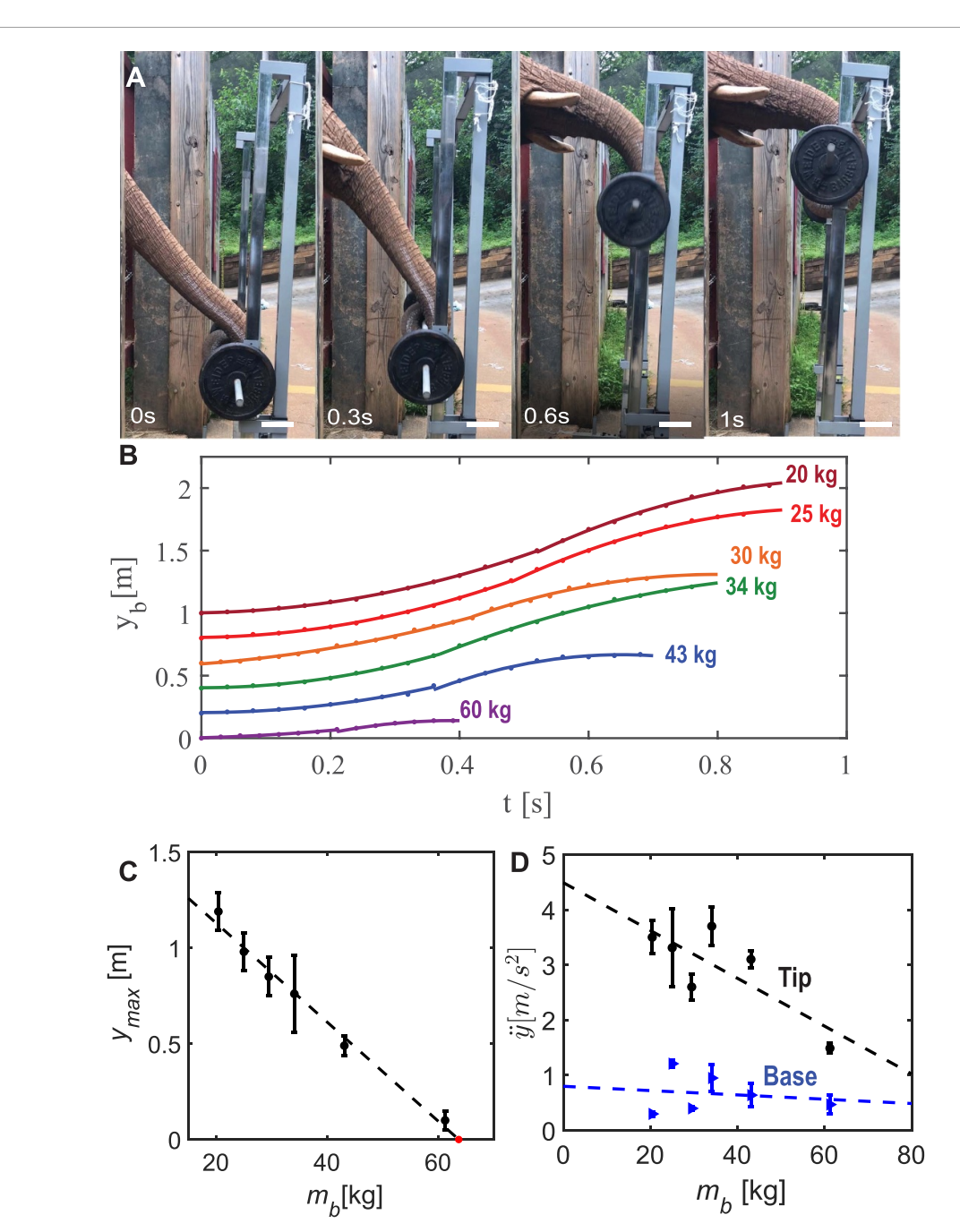


Figure 2. Kinematics of weight lifting. (a) Time series of the elephant lifting a barbell at increments of 0.3 s with scale bars showing 10 cm. (b) Time course of the position of the barbell, with trajectories staggered for clarity. Weights include: maroon (20 kg), red (25 kg), orange (30 kg), green (34 kg), blue (43 kg), purple (60 kg). Solid lines are best fit lines associated with constant acceleration *a* and constant deceleration. (c) Relationship between maximum height of the elephant trunk and the barbell mass. A red dot indicates the x-intercept, which is the prediction of the maximum mass that the elephant can lift in this setup. (d) Relationship between vertical acceleration and barbell mass. The tip and the base of the trunk are shown by black circles and blue triangles, respectively. Best fits given by the dashed lines.

measurements, the inner and outer radii for the trunk tip are r(0) = 1.1 cm and R(0) = 2.2 cm, respectively. The nasal passages of the frozen trunk were squashed by self-weight. We used the nasal circumference to extrapolate the inner radius (figure 4(d)).

3.2. Tension and power applied

To determine the force required to lift the barbell, we consider a vertical force balance on the trunk tip. A control volume is shown schematically in figure 5(a).

When the barbell is lifted, the elephant lifts both the barbell and the trunk itself. The total mass to be lifted is $m = m_t + m_b$ where m_b is the barbell mass and m_t is the mass of the trunk segment in contact with the barbell. In reality, the proximal portion of the trunk rises as well. However, the average height of the trunk segments not in contact cannot be easily calculated since part of the elephant trunk leaves the video frame. Thus, a weakness of our method is that the applied force and power will be underestimated. To

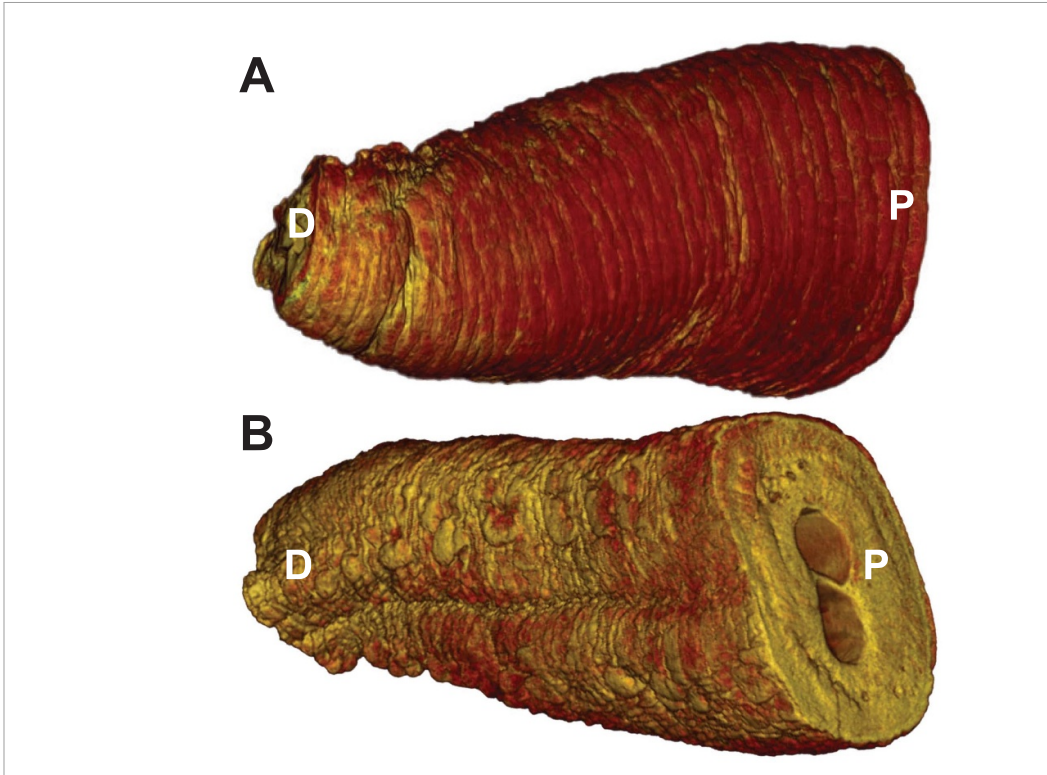


Figure 3. CT scan of the trunk of a 38 year old female African elephant *Loxodonta africana*. (a) Dorsal section and (b) ventral section. P refers to proximal (towards the skull), D refers to distal (towards the tip). The section shown is the distal 60 cm of the trunk.

determine the vertical acceleration at the base of the trunk, we measured the vertical position of the apex of the tusk, which stayed within the video frame.

The trunk exerts a tension T to lift. The angle ϕ between the trunk and the horizontal is measured at the instant the lift begins (figure 5(a)). We neglect the displacement in the horizontal direction because the Smith Machine constrains the barbell from moving horizontally. Since the trunk segment is wrapped around the barbell, both move with the same vertical speed \dot{y} and acceleration \ddot{y} . By Newton's law, the vertical force balance may be written

$$m\ddot{y} = -mg + T\sin\phi,\tag{2}$$

where g is the acceleration of gravity and T is the tension applied. Solving equation (2) with respect to the tension force T yields

$$T = \frac{m(\ddot{y} + g)}{\sin \phi}. (3)$$

Thus, by measuring the angle ϕ and the acceleration \ddot{y} , we can estimate the force exerted to lift the barbell.

We calculate the power to lift the tip and the base of the trunk. Each of these parts has its own mass that is estimated from equation (1). The average power exerted to lift part i of the trunk may be written as the ratio of the gravitational potential energy and duration t of lift. The gravitational potential energy of a trunk segment of mass m_i is written as $U = m_i g y_i$,

where y_i is the change in the height of the center of mass of that portion of the trunk. The mass of the tip was assumed to be between 5.4 and 9 kg, depending on the observation of the length of wrap. The mass of the trunk base was assumed to be 60 kg, which we give as an upper bound. The power is thus

$$P_i = \frac{m_i g y_i}{t},\tag{4}$$

which is consistent with the definition of power for human weight lifters [25].

3.3. Contact area

While the dorsal trunk is cylindrical, the ventral part of the trunk is planar and covered with wrinkles. To estimate the contact area of the trunk and the barbell, we measure the frequency ω and amplitude Aof the trunk wrinkles at 80 positions, including eight axial positions along the frozen elephant trunk and 10 azimuthal positions for each axial position. Previous work showed that the trunk tip is nearly inextensible: the distal 30 cm of the trunk stretches less than 10% strain, which is small compared to the 25% stretch mid-distally [12]. We thus assume that the wrinkle geometry of the frozen trunk matches the live elephant. Assuming a sinusoidal wrinkle profile, the radius R of the ventral trunk skin as a function of distance z from the tip is written in the results section in equation (15).

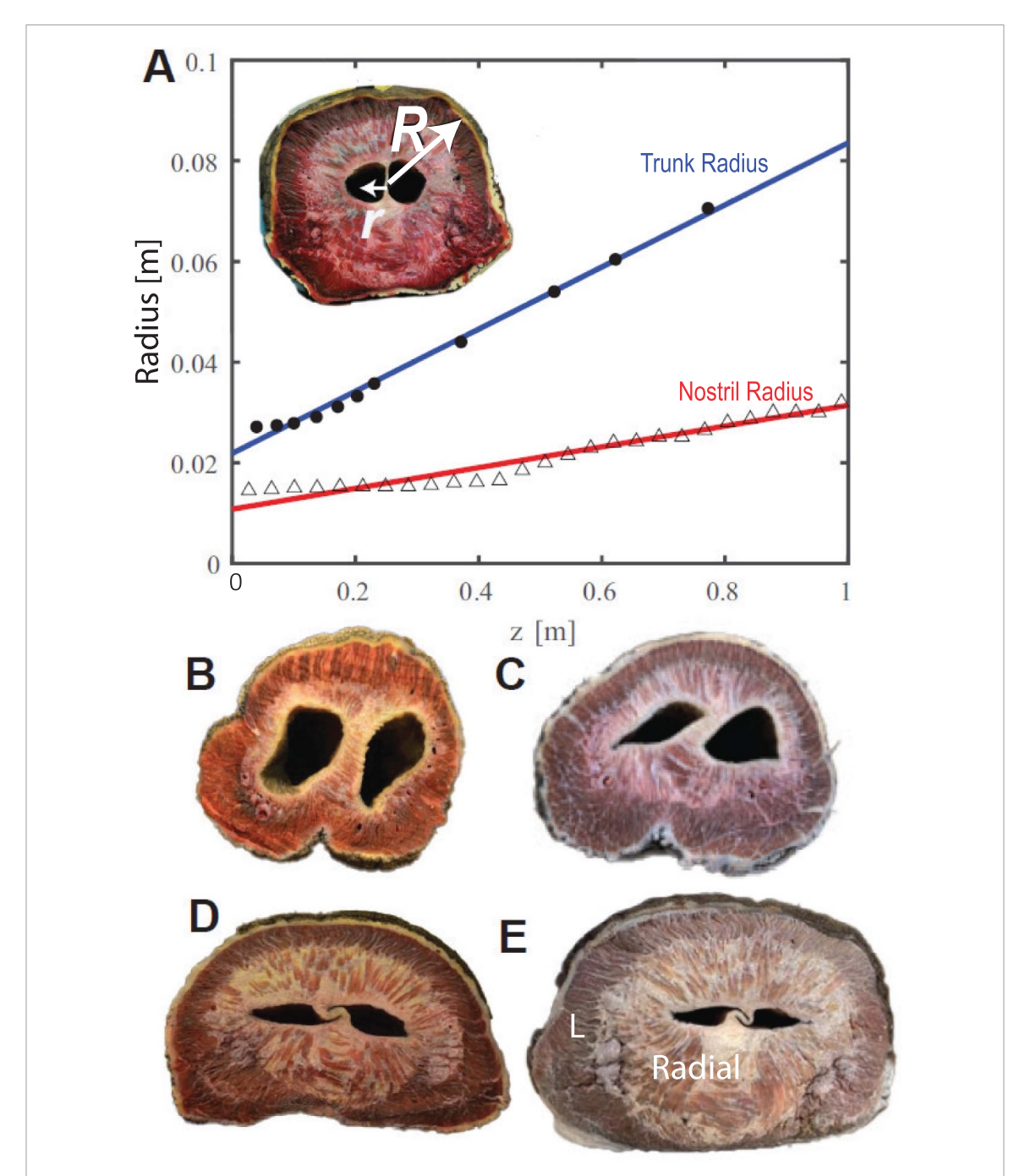


Figure 4. Elephant trunk anatomy. (a) The relationship between radii of the trunk and distance z from the tip. The trunk outer radius R is given by the shaded circles, and inner nasal radius r by open triangles. Linear best fits are shown by the solid lines. (b)–(e) Elephant trunk cross sections displaying muscle fibers and negative space created by nasal passageway. (b) Cross section 28 cm from distal tip. (c) 56 cm from distal tip. (d) 100 cm from distal tip. (e) 140 cm from distal tip with 'L' indicating longitudinal muscles, and 'radial' indicating radial muscles.

We report the amplitude A(z) and frequency $\omega(z)$ in the results section and in figures 7(e) and (f). To calculate the surface area of contact of a trunk segment, we utilize the arclength formula which states the arclength s of the trunk segment is

$$s = \int_{z=z_0}^{z=z_f} \sqrt{1 + \left(\frac{dR}{dz}\right)^2}.$$
 (5)

This integral is calculated numerically using MAT-LAB ode45, between the two points z_0 and z_f , which

defines the trunk segment in contact with the bar. We assume the contact region is a wrinkled planar trapezoid of height s, and lengths $D(z_f)$ and $D(z_0)$, which are the diameters of the trunk at the points z_f and z_0 . The area of this trapezoid is:

$$SA = \frac{1}{2}s(D(z_f) + D(z_0)),$$
 (6)

where we used as an upper bound the entire wrinkle surface area that contacts the bar.

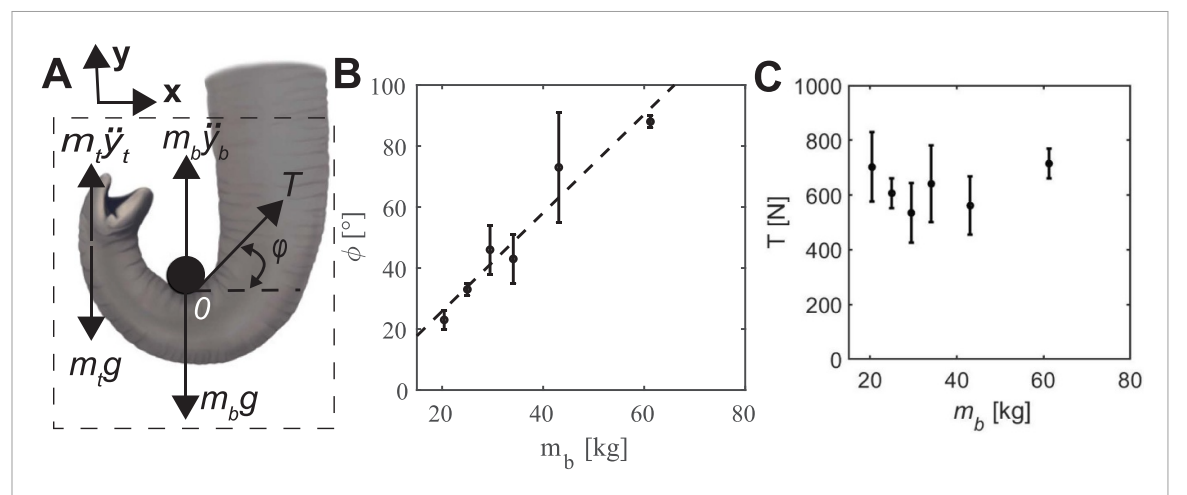


Figure 5. Forces exerted on the barbell. (a) Free body diagram of the elephant lifting a barbell. At contact point O, the elephant applies a tension T to the barbell to lift. The trunk is at an angle of contact ϕ with respect to the horizontal. The combined trunk and barbell mass experiences gravity g and an upward acceleration \ddot{y} . (b) The relationship between the angle of contact ϕ and barbell mass. Linear best fit is given by the dashed line. (c) The relationship between the calculated tension T and barbell mass.

4. Results

4.1. Trunk geometry

To calculate the force applied by the trunk, we first measure its shape. We characterize the frozen trunk from the Smithsonian using CT-scanning and dissection (figure 3, supplemental video 4). At the proximal base, the cross-section is dominated by radial muscle, marked 'radial,' the light-colored muscle close to the nasal cavities. A large amount of radial muscle is presumably to help with lifting as the base does not stretch much longitudinally (figure 4(e)) [12]. The longitudinal muscle marked 'L,' is darker red and lies between the radial muscle and the skin of the trunk. The proportion of radial muscle shrinks progressively towards the distal tip, while the proportion occupied by the nostrils increases. The distal tip of the trunk lacks radial muscle and is instead dominated by two oblique muscle groups (figure 4(b)), which assist with wrapping around objects.

The trunk is a hollow conical frustum permeated by a pair of nostrils. From the CT scans, we obtain a relationship for both the inner and outer radius of the trunk at a distance from the tip, z (figure 4(a)). The inner radius r is given by the open triangles and the outer radius R by the closed points. The solid lines are linear least squares best fits given by

$$r(z) = 0.011 + 0.0002z, (R^2 = 0.95),$$
 (7)

$$R(z) = 0.022 + 0.0006z, (R^2 = 0.99),$$
 (8)

with all units in meters. At the tip, the inner and outer radii are 1.1 cm and 2.2 cm. At a point 100 cm from the tip, the trunk has inner and outer radii of 3 cm and 8 cm. Using equation (1), we calculate a trunk mass of 97 kg, which is close to the experimental

measurement of 110 kg. The mass m_t of the trunk segment in contact with the barbell was calculated for each experiment based on the length in contact. The mass of the trunk in contact ranged from 5.4 kg for the lightest barbell up to 9.0 kg for the heaviest.

4.2. Lifting force

The elephant lifts the barbell by first wrapping its trunk tightly around it (figure 1). The trunk arches like a bending beam as it lifts (figure 2(a) and supplemental video 1–3). The total energy expended for each barbell weight is related to the maximum height of the lift y_{max} , shown in figure 2(c). The linear best fit, shown by the dashed line, is

$$y_{\text{max}} = 1.64 - 0.026 m_b, (R^2 = 0.95)$$
 (9)

where $y_{\rm max}$ is the height lifted in meters. For this and future equations, m_b is the weight of the barbell in kg. The elephant lifted the lightest weight to a height of 1.19 ± 0.1 m (n=4), nearly touching the top of the weight rack, and the heaviest weight to less than one-tenth the height at 0.1 ± 0.05 m (n=2). Clearly, the elephant lifted heavier weights less. The x-intercept of equation (9) shows that that the heaviest weight that elephants can lift in this setup is 63 kg, which is just 2% of its body weight and 65% of its trunk weight. This weight is less than we expected given an elephant's feats of strength. We surmise that the barbell apparatus constrained the trunk motion to the vertical, preventing the elephant from using body weight to push or lift the object.

The time course of the barbell height y_b is shown in figure 2(b), where we spaced out the trajectories for clarity. After the trunk wrapped around the barbell, the lifts were fast, taking approximately 0.5–0.8 s across the weight classes. Each function was fit

with two quadratic best fits separated by an inflection point between the acceleration and deceleration phases. The inflection point usually occured at the midpoint of the lift. In the acceleration phase, the position may be written as $y_b = at^2$ where t is time, and a is the acceleration. This equation describes lifting from a rest position with a constant acceleration a. Such a relationship fits the acceleration phase well, with an R^2 greater than 0.95. The deceleration phase was fit with the position and velocity at the inflection point, as well as a constant deceleration: $y_b = y_0 + vt - bt^2$. We found no clear trend between deceleration and barbell mass, so the deceleration was not reported. The fits for the entire lift are shown in figure 2(b). The acceleration $\ddot{y_b} = a$ for each barbell mass is shown in figure 2(d), with the linear best fit given by

$$\ddot{y}_b = 4.49 - 0.043 m_b, (R^2 = 0.63),$$
 (10)

where \ddot{y}_b is in m s⁻² and m_b is in kg. Equation (10) indicates that an elephant has a lower acceleration for heavier weights: acceleration ranges from 3.9 m s⁻² for the lowest weight to less than half that value for a weight three times heavier.

Closer to the elephant's head, lifting is accomplished by some combination of rotation and lifting of the head. The blue points in figure 2(d) shows the vertical acceleration of the trunk base: the acceleration of $1~{\rm m\,s^{-2}}$ is small compared to the trunk tip accelerations shown in black. We conclude that vertical motion is small, and instead, the neck acts like a fulcrum to provide rotational motion to assist lifting by the trunk tip.

To calculate the tension applied by the trunk, we measured the angle that the trunk intersects the barbell. Figure 5(b) gives the angle ϕ of the trunk with respect to the horizontal, where the dashed line is the least squares linear best fit. The relationship between the angle of the trunk and barbell mass is

$$\phi = -6.4 + 1.6m_h, (R^2 = 0.94),$$
 (11)

with ϕ in degrees. An angle of 90° indicates that the elephant orients its trunk vertically. The elephant increases the angle of contact ϕ from $23 \pm 3^\circ$ (n=4) for the lightest weight to nearly four times that amount, or $89 \pm 2^\circ$ (n=2), for the heaviest.

Given the angle ϕ and the length of the trunk z wrapped around the bar, we calculate the trunk tension T using equation (3) in the Math Methods. The relationship between tension and the mass lifted is shown in figure 5(c). Although the barbell weights increase by a factor of three, the tension increases by only 20%, maintaining an average value of 620 ± 64 N (n = 22) across all trials. We thus see that elephants

have dual 'strategies' to maintain tension when lifting heavy weights: they decrease acceleration and orient their trunk more vertically. These strategies may not be volitional: they may simply arise from trying to lift a heavier weight with a finite muscle of limited force and power. Nevertheless, we see the trunk adapts to different postures and kinematics for different weights.

Figure 6(b) shows the relationship between power exerted and the mass lifted, with red points referring to the trunk base and black points to the trunk tip. These powers are overestimated because they only consider the maximum deflection of the highest point rather than the center of mass of each section. The power expenditure of the tip is U-shaped, with a peak power of 357 ± 79 W (n=4) for intermediate masses. No matter what weight is lifted, the power expended at the trunk base remains higher than the trunk tip. This is because the mass of the base is 60 kg whereas the mass of the tip is less than 10 kg.

4.3. Prehension

Although the elephant was at a constant distance to the bar, it wrapped a greater length of its trunk to lift heavier weights. Figure 6(a) shows the progression of trunk wrapping, from $\theta=87\pm6^\circ$ (n=4) to $400\pm12^\circ(n=2)$, an increase in wrapping angle of 400%. To lift the lightest weights $(m_b=20$ and 25 kg), the trunk's distal tip extended past the barbell and wrapped around the bottom half, creating a lip that kept the barbell in place. When lifting medium weights $(m_b=30\text{--}43\text{ kg})$, the trunk extend further, using a thicker section of its trunk to wrap. Finally, when the elephant lifted the heaviest weight $(m_b=60\text{ kg})$, the trunk wrapped 413° or more than a full cycle.

Wrapping a greater angle increases the contact area between the barbell and the elephant trunk. We note that the largest angle supporting the barbell's weight is 180°, corresponding to the bottom half of the barbell. Any additional wrapping helps with stability rather than weight support.

For us to rationalize the increased wrapping angle with heavier weights, we consider the capstan, a rotating device that amplifies a sailor's ability to pull a rope [26]. The classical capstan model shows that $T_b/T_a=e^{-\mu\theta}$ where θ is the angle subtended by the capstan, μ is the coefficient of friction, and T_b/T_a is the ratio of the sailor's force to the force on the other end of the rope. Assisted by the friction on the rope wrapped around the capstan, the sailor can amplify its force T_b to support a load T_a .

Applying the capstan problem to the barbell wrapping, we may consider the 'sailor' to be $T_b = m_t g$, which is the gravitational force imposed by the trunk pendent mass m_t wrapped around the barbell. The

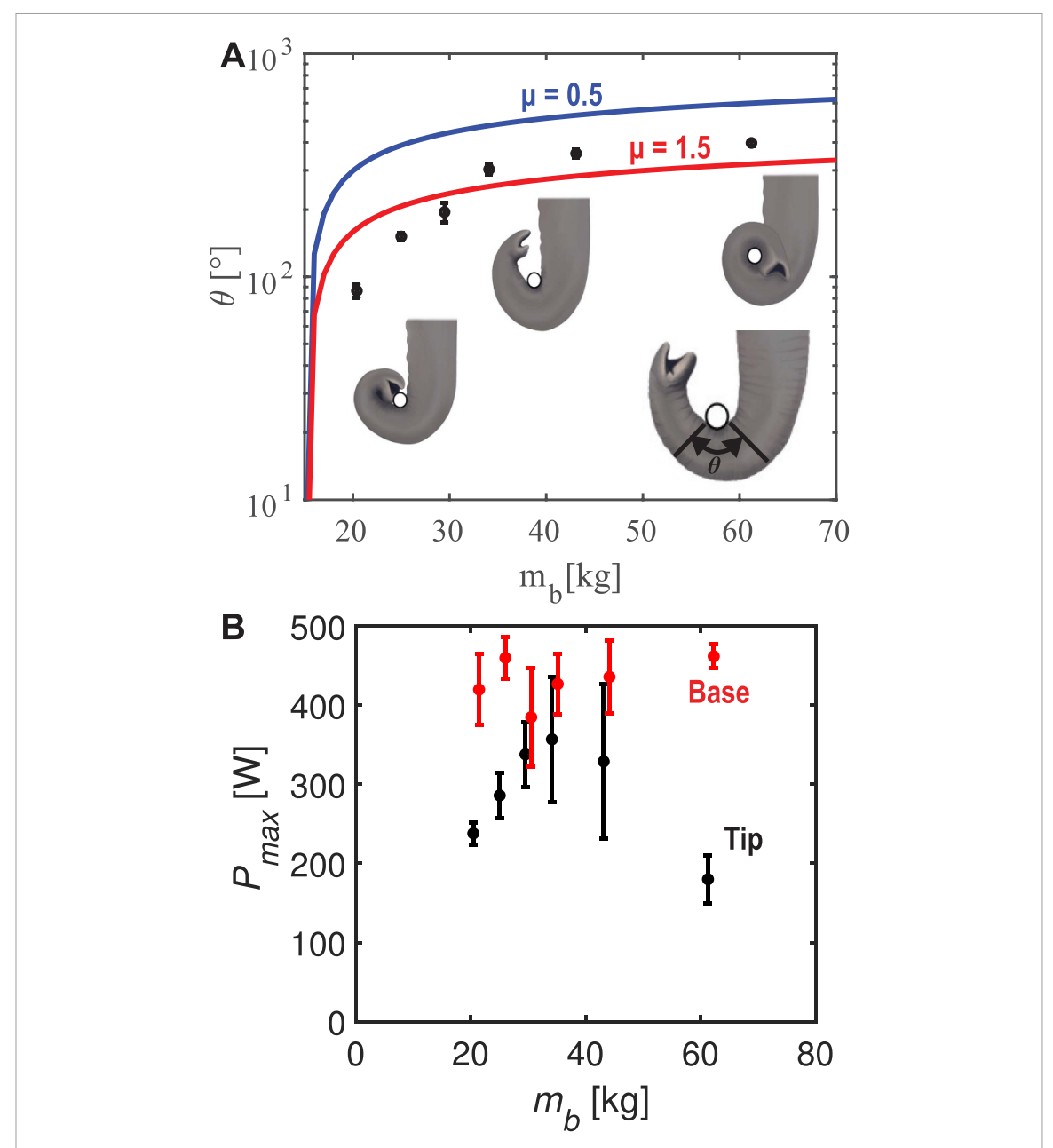


Figure 6. Elephants wrap the trunk to lift heavier weights. (a) The relationship between angle of trunk wrap θ and barbell mass. Schematics, from left to right, show the increasing wrap of the trunk for barbell weights 20 kg, 25 kg, and 60 kg. Theoretical predictions with friction coefficients of 0.5 and 1.5 are shown by the blue and red lines, respectively. (b) Maximum power exerted to lift different barbell masses. Power is calculated at two locations, the distal tip (black circles) and the proximal root (red circles).

weight of the pendnt, as well as the friction at the contact area, opposes the barbell weight $T_a = m_b g$. By wrapping greater angles, the elephant can use the weight of the pendant to avoid losing grip on the barbell as it is lifted. Based on the arclength of the trunk wrapped, the weight of the pendent mass varies from 5.4 to 9 kg and increases with barbell mass. Simplifying the capstan model, we find

$$\theta = a \ln \left(b m_b \right) \tag{12}$$

where $a = \frac{1}{\mu}$ and $b = \frac{1}{m_t}$. A least-square best fit, given in red, fits the data quite well, showing that $100^{\circ}-300^{\circ}$ of wrap is sufficient to hold the barbell

(figure 6(a)). The free parameter for the best fit is a high but still physically reasonable friction coefficient of $\mu=1.5$, comparable to the friction coefficient of 1.6 for bio-mimetic snake robots scales on styrofoam [22]. Snakes can change the angle of their ventral scales to increase frictional forces as they climb tree trunks and other vertical surfaces. Such actively deformable surfaces are analogous to the friction-enhancing wrinkles and coarse hair on the trunk. For comparison, we show in blue another wrapping angle using the friction coefficient of human skin on metal ($\mu=0.8$). Indeed, such a low friction coefficient requires 200°–500° wrapping angles, which are higher than observed. Both models bound the

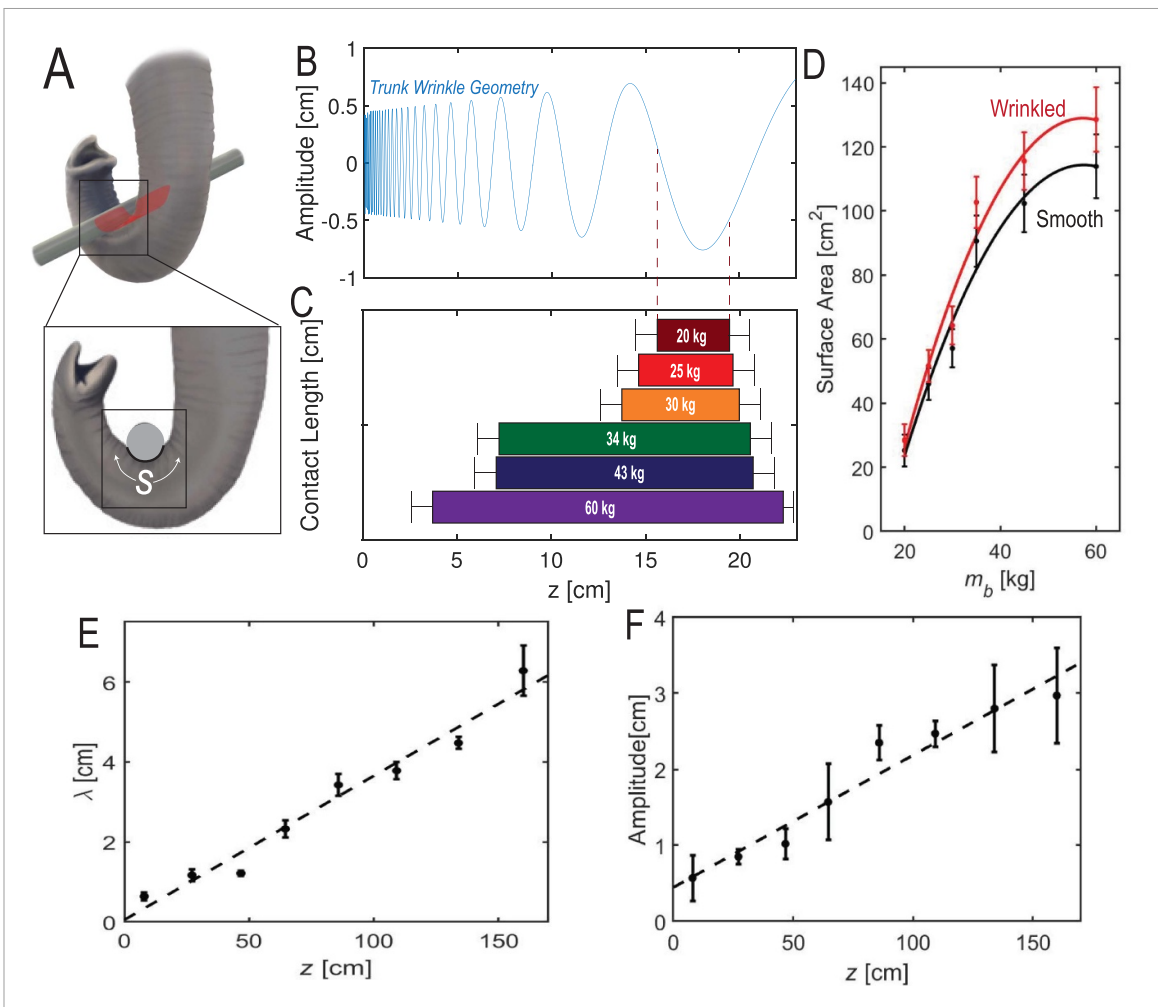


Figure 7. Elephant wrinkles increase area of contact with the barbell. (a) Schematic displaying the elephant's area of contact with the barbell using its wrinkled ventral trunk. (b) Ventral surface profile along the trunk's long axis. Wrinkles increase in amplitude and wavelength with distance from the tip, which is at z=0. (c) Observed contact length s of the barbell for different barbell weights. This length does not take into account wrinkles. (d) Surface area of contact across weight classes, with black showing the surface area without wrinkles, and red the surface area with wrinkles. (e) Wavelength of the elephant wrinkles from the tip of the trunk to the base. (f) Amplitude of the elephant wrinkles from the tip of the trunk to the base.

data and give evidence that the combination of the pendant weight and skin friction prevent the barbell from slipping as it is lifted.

Our capstan model assumed a constant friction coefficient, but the trunk may be able to modify its friction coefficient using its wrinkled grip, as shown in figure 7(a). We measured by hand the wrinkle amplitude A and wavelength λ as a function of the distance z from the tip. A linear least squares best fit shows that wrinkles increase in amplitude and wavelength with distance from the tip:

$$A(z) = 0.0174z + 0.4461(R^2 = 0.95)$$
 (13)

$$\lambda(z) = 0.036z + 0.051(R^2 = 0.97)$$
 (14)

(figures 7(e) and (f)) where A, λ , and z are in cm. Assuming that the trunk surface has a sinusoidal wrinkle pattern, the wrinkle height may be written

$$y_{\text{wrinkle}} = A(z)\sin\frac{2\pi}{\lambda(z)}z,$$
 (15)

and is shown in figure 7(b). Using these relationships, we use equation (6) to estimate the surface area of the wrinkled skin. As the barbell mass increases, the elephant wraps with increased arc length and greater surface area (figure 7(c)). We consider two estimates of its surface area. First, we consider a smooth ventral trunk devoid of wrinkles, shown by the black points (figure 7(d)). An upper bound for the increase in surface area is that the entire wrinkle, including the peaks and troughs, are wrapped around the bar: The wrinkled surface area, from equation (6) is shown in red. In reality, the peaks will be compressed, and there will be air gaps in the troughs of the wrinkles. However, further analysis is not feasible without measuring the contact area precisely. The true contact area will likely between the black and red curves. Low wrapping angles create little additional surface area because the trunk tip's wrinkles are small. Large degrees of wrapping may involve deeperwrinkles that contribute up to 15% additional surface area (figure 7(d)).

5. Discussion

Although the Smith Machine was designed for human weight lifting, it worked for elephants because the power generated by the elephant trunk is comparable to human power. When humans lift a barbell for a power clean, which involves lifting a barbell from the ground to the shoulders, they can achieve a power of 900 W on free weights, and 770 W on machine cleans for lifting just a 20 kg weight [25]. When using just its trunk, the elephant lifts 20 kg using only 238 ± 14 W of power, but could probably increase this amount with training.

To lift heavier weights, the elephant recruits a greater surface area of contact using its trunk wrinkles. The ridges on human fingertips have been shown to increase friction by two mechanisms [27]. On rough surfaces, the ridges deform and interlock into an uneven surface when gripping surfaces. Our videography was not close enough to observe any deformation of the wrinkles. However, the mechanism seems plausible since elephants often pick up rough objects such as tree bark, whose asperities on the mm to cm seem comparable to those of elephant wrinkles. The other mechanism for human fingertips is more subtle, involving the maintenance of an optimal layer of sweat between the ridges. The length scale of elephant wrinkles is much larger than human fingertip ridges; moreover, elephants have very few sweat glands [28]. Therefore it is unlikely that moisture plays a role in elephant grip.

The use of wrinkles to increase contact area may be useful for improving the grip of soft robots. Artificial muscles composed of silicon elastomers can actuate rigid grippers to pick up objects. One artificial muscle, known as hydraulically amplified self-healing electrostatic actuators (HASEL) [15], can grasp various objects and use its own feedback to estimate the object's size [29]. Fluid-filled toroidal tubes can grip, catch, and convey objects [30]. Generally, such robots are covered in smooth skin. The addition of wrinkles [12] may improve grip without increasing the squeeze force and damaging fragile objects. The wrinkles may also improve the devices' reach by enabling the skin to stretch. Uncontrolled grippers that rely on the entanglement of filaments could also be covered in wrinkles to improve grip [31]. One day, wrinkled skin could also improve the ability of soft robots to perform sensing. Adding smooth artificial skin to earthworminspired robots facilitated feedback control [20]. The addition of wrinkles may enable a more stretchable interface with its subterranean environment.

Many aspects of elephant trunk lifting remain poorly understood. In many prehensile animals, the surface of the skin is heavily innervated with sensors. Elephant skin is substantially tougher than other animals but somehow maintains a sensitive touch. Since our experiments were performed with only one elephant of one sex, further work is needed to generalize our observations across elephant species. African and Asian elephants differ in their trunk anatomy in that African elephants are browsers, and Asian elephants are grazers. This specialization gives African elephants two prehensile trunk fingers, whereas Asian elephants have one, which leads to differences in facial motor control neurons [14].

6. Conclusion

In this study, we elucidate the kinematic and gripping strategies of an elephant lifting a barbell. As the barbell increased in weight, the elephant maintained nearly constant tensile force by orienting its trunk vertically and accelerating less. The elephant wrapped its trunk around the bar more for heavier weights, presumably to stabilize its grip. We showed that the self-weight of the trunk might be used like a sailor's capstan to prevent slipping of the barbell. Incorporating a greater length of the trunk also brings into play deeper and longeramplitude wrinkles, which we believe increase friction. Since one elephant was studied, it remains unknown whether these results generalize to other lifted objects or other elephants. We hope that this work inspires new kinds of adaptable biologically inspired grippers.

Data availability statement

The data that support the findings of this study are openly available at the following URL/DOI: https://github.com/Aschulz94/SchulzWrapping.

Acknowledgments

This work was supported by the US Army Research Laboratory and US Army Research Office Mechanical Sciences Division Complex Dynamics and Systems Program, under Contact Number W911NF-12-4-00111. We thank A Lee, M Chan, and Y Zhang for their early contributions. We thank the Zoo Atlanta elephant keepers with their assistance in performing experiments. We thank Dr Ali Nabaviziadeh for arranging the collaboration with Dr Reidenberg. We thank the imaging time donated by Dr Cheuk Tang's group, Radiology, Neuroscience, & Psychiatry Translation and Molecular Imaging Institute at Icahn School of Medicine at Mount Sinah. We thank J Ososky and the Smithsonian Institution Museum of Natural History for their assistance with information regarding the frozen elephant trunk as well as loaning the elephant trunk to Icahn School of Medicine at Mount Sinah.

Conflict of interest

The authors declare no conflicts of interest in any of this manuscript.

Data access statement

We have included MATLAB files for the elephant lifts, raw elephant lifting trials, and data spreadsheets of strain tracking available for download on a Git-Hub repository that is linked in the supplemental documents.

Ethics statement

In working with animals from Zoo Atlanta. We received research permits from both Zoo Atlanta, permit name, *Weight lifting experiments by elephants*, and Georgia Institute of Technology IACUC, Permit Number A16032.

Funding statement

D L H, A K S, J N W were supported by the US Army Research Laboratory and the US Army Research Office Mechanical Sciences Division, Complex Dynamics and Systems Program, under Contract Number W911NF-12-R-0011.

ORCID iDs

Andrew K Schulz https://orcid.org/0000-0001-8007-5157

Joy S Reidenberg https://orcid.org/0000-0002-4180-7156

Jia Ning Wu https://orcid.org/0000-0003-0902-

Benjamin Seleb https://orcid.org/0000-0001-5023-1972

David L Hu https://orcid.org/0000-0002-0017-7303

References

- [1] Jones-Engel L E and Bard K A 1996 Precision grips in young chimpanzees Am. J. Primatol. 39 1–15
- [2] Wilson J F, Mahajan U, Wainwright S A and Croner L J 1991 A continuum model of elephant trunks J. Biomech. Eng. 113 79
- [3] Schulz A K, Wu J N, Ha S Y S, Kim G, Slade S B, Rivera S, Reidenberg J S and Hu D L 2021 Suction feeding by elephants J. R. Soc. Interface 18 20210215
- [4] Wu J, Zhao Y, Zhang Y, Shumate D, Slade S B, Franklin S V and Hu D L 2018 Elephant trunks form joints to squeeze together small objects J. R. Soc. Interface 15 20180377
- [5] Dagenais P, Hensman S, Haechler V and Milinkovitch M C 2021 Elephants evolved strategies reducing the biomechanical complexity of their trunk *Curr. Biol.* 31 4727–37.e4
- [6] McGinn C 2015 Prehension: The Hand and the Emergence of Humanity (Cambridge, MA: MIT Press)
- [7] Emmons L H and Gentry A H 1983 Tropical forest structure and the distribution of gliding and prehensile-tailed vertebrates Am. Nat. 121 513–24
- [8] Laska M 1998 Laterality in the use of the prehensile tail in the spider monkey (*Ateles geoffroyi*) Cortex 34 123–30
- [9] Laska M 1996 Manual laterality in spider monkeys (Ateles geoffroyi) solving visually and tactually guided food-reaching tasks Cortex 32 717–26

- [10] Organ J M, Muchlinski M N and Deane A S 2011 Mechanoreceptivity of prehensile tail skin varies between ateline and cebine primates *Anatomical Rec.* 294 2064–72
- [11] Russo G A and Young J W 2011 Tail growth tracks the ontogeny of prehensile tail use in capuchin monkeys (*Cebus albifrons* and *C. apella*) Am. J. Phys. Anthropol. 146 465–73
- [12] Schulz A K, Boyle M, Boyle C, Sordilla S, Rincon C, Hooper S, Aubuchon C, Reidenberg J S, Higgins C and Hu D L 2022 Skin wrinkles and folds enable asymmetric stretch in the elephant trunk *Proc. Natl Acad. Sci.* 119 e2122563119
- [13] Iberall T 1997 Human prehension and dexterous robot hands Int. J. Robot. Res. 16 285–99
- [14] Kaufmann L V, Schneeweiß U, Maier E, Hildebrandt T and Brecht M 2022 Elephant facial motor control *Sci. Adv.* 8 eabq2789
- [15] Rothemund P, Kellaris N, Mitchell S K, Acome E and Keplinger C 2021 HASEL artificial muscles for a new generation of lifelike robots—recent progress and future opportunities Adv. Mater. 33 2003375
- [16] Wilson J F, Li D, Chen Z and George R T 1993 Flexible robot manipulators and grippers: relatives of elephant trunks and squid tentacles Robots and Biological Systems: Towards a New Bionics? (Nato ASI Series) ed P Dario, G Sandini and P Aebischer (Berlin: Springer) pp 475–94
- [17] Scott G P, Henshaw C G, Walker I D and Willimon B 2015 Autonomous robotic refueling of an unmanned surface vehicle in varying sea states 2015 IEEE/RSJ Int. Conf. on Intelligent Robots and Systems (IROS) (Hamburg, Germany) (IEEE) pp 1664–71
- [18] Hannan M W and Walker I D 2003 Kinematics and the implementation of an elephant's trunk manipulator and other continuum style robots J. Robot. Syst. 20 45–63
- [19] Booth J W, Shah D, Case J C, White E L, Yuen M C, Cyr-Choiniere O and Kramer-Bottiglio R 2018 OmniSkins: robotic skins that turn inanimate objects into multifunctional robots Sci. Robot. 3 eaat1853
- [20] Calderón A A, Ugalde J C, Chang L, Cristóbal Zagal J and Pérez-Arancibia N O 2019 An earthworm-inspired soft robot with perceptive artificial skin *Bioinspir. Biomim.* 14 056012
- [21] Marvi H, Cook J P, Streator J L and Hu D L 2016 Snakes move their scales to increase friction *Biotribology* 5 52–60
- [22] Marvi H, Meyers G, Russell G and Hu D L 2011 Scalybot: a snake-inspired robot with active control of friction ASME 2011 Dynamic Systems and Control Conf. and Bath/ASME Symp. on Fluid Power and Motion Control (Arlington, Virginia, USA) vol 2 (ASMEDC) pp 443–50
- [23] Read W T 1937 Handbook of Engineering Fundamentals (Eshbach, Ovid W., ed.) J. Chem. Educ. 14 49
- [24] Kern W F and Bland J R 1954 Solid Mensuration With Proofs 2nd edn (New York: Wiley) (available at: https://doi.org/ ark:/3960/t7vm9nf94)
- [25] Jones R M, Fry A C, Weiss L W, Kinzey S J and Moore C A 2008 Kinetic comparison of free weight and machine power cleans J. Strength Cond. Res. 22 1785–9
- [26] Gao X, Wang L and Hao X 2015 An improved Capstan equation including power-law friction and bending rigidity for high performance yarn Mech. Mach. Theory 90 84–94
- [27] Yum S-M et al 2020 Fingerprint ridges allow primates to regulate grip Proc. Natl Acad. Sci. 117 31665–73
- [28] Wright P and Luck C 1984 Do elephants need to sweat? South Afr. J. Zool. 19 270–4
- [29] Yoder Z, Macari D, Kleinwaks G, Schmidt I, Acome E and Keplinger C 2022 A soft, fast and versatile electrohydraulic gripper with capacitive object size detection Adv. Funct. Mater. 33 2209080
- [30] Root S E, Preston D J, Feifke G O, Wallace H, Alcoran R M, Nemitz M P, Tracz J A and Whitesides G M 2021 Bio-inspired design of soft mechanisms using a toroidal hydrostat Cell Rep. Phys. Sci. 2 100572
- [31] Becker K, Teeple C, Charles N, Jung Y, Baum D, Weaver J C, Mahadevan L and Wood R 2022 Active entanglement enables stochastic, topological grasping *Proc. Natl Acad. Sci.* 119 e2209819119